



HAL
open science

Analysis of Current-Voltage Characteristics in Insulating Polymers using a Bipolar Charge Transport Model

S. Le Roy, Fulbert Baudoin, C. Laurent, G. Teyssedre

► To cite this version:

S. Le Roy, Fulbert Baudoin, C. Laurent, G. Teyssedre. Analysis of Current-Voltage Characteristics in Insulating Polymers using a Bipolar Charge Transport Model. *IEEE Transactions on Dielectrics and Electrical Insulation*, 2022, 10.1109/TDEI.2022.3217429 . hal-03853031

HAL Id: hal-03853031

<https://hal.science/hal-03853031>

Submitted on 15 Nov 2022

HAL is a multi-disciplinary open access archive for the deposit and dissemination of scientific research documents, whether they are published or not. The documents may come from teaching and research institutions in France or abroad, or from public or private research centers.

L'archive ouverte pluridisciplinaire **HAL**, est destinée au dépôt et à la diffusion de documents scientifiques de niveau recherche, publiés ou non, émanant des établissements d'enseignement et de recherche français ou étrangers, des laboratoires publics ou privés.

Analysis of Current-Voltage Characteristics in Insulating Polymers using a Bipolar Charge Transport Model

S. Le Roy, F. Baudoin, C. Laurent, and G. Teyssedre

Abstract— A bipolar charge transport model has first been used to compare the current voltage characteristics (J-E) for different applied voltage protocols and different times under voltage taking low density polyethylene as a case study, as a steady state may take a very long time to be reached experimentally. Simulation results highlight the necessity to spend substantial time under voltage to reach a quasi-stable current. In a second part, evolutions of the model in terms of physical processes are proposed, to observe their impact on the J-E characteristics, and particularly the appearance of electric field thresholds, as proposed by the Space Charge Limited Current (SCLC) theory. To do so, different mathematical expressions are proposed for each physical process related to injection, mobility and trapping. Field dependent mobility equations allow obtaining electric field threshold values comparable to experimental data, while a constant mobility is the only way to observe a trap free limit region. Moreover, all parameters linked to trapping are of most importance in the observation of a SCLC characteristic, but are not enough to observe a trap free limit region when electric field dependent mobility is considered.

Index Terms— bipolar charge transport model, fluid model, J-E characteristics, polymer insulation, SCLC theory

I. INTRODUCTION

CURRENT-voltage measurements are necessary to characterize polymers used as electrical insulation under direct current (DC) thermo-electrical stress. They are often analyzed in terms of Space Charge Limited Current (SCLC) theory. This theory has been developed with simple but restrictive physical hypotheses [1], such as one type of carrier, ohmic contacts, no traps or a unique level of traps, and steady state condition. Figure 1 illustrates a typical current density as a function of voltage curve, where different regions are observed:

- an Ohmic region, where $J \propto V$. This region is often not observed experimentally for insulating polymers.
- A trap limited current region, where $J \propto V^2$ when traps are not distributed
- A trap-filled limited current, i.e. $J \propto V^\infty$, where theoretically a single trapping level is considered. When traps (deep traps particularly) are distributed, the slope is not infinite.
- A trap free limited current. The voltage at which all traps are filled is called V_{TFL} .

Even with such restrictive physical hypotheses, the SCLC theory

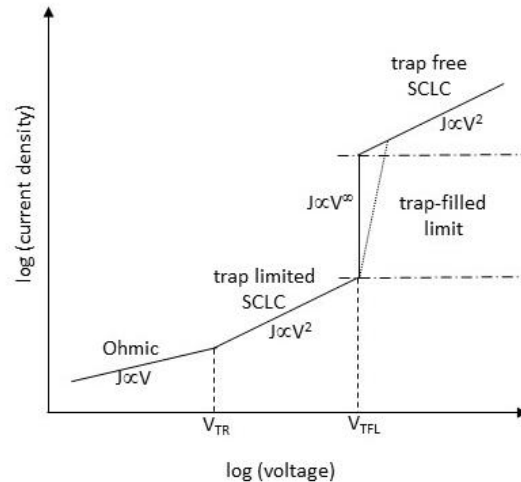


Fig. 1. A typical current density-voltage characteristic of space-charge-limited conduction current. V_{TR} is transition voltage. V_{TFL} is trap-filled limit voltage.

allows describing the specific S-shaped current density-voltage (J-V), or current density-electric field (J-E) characteristic often observed for insulating polymers [2], and particularly polyethylene [3]. Among the restrictive physical hypotheses of the SCLC theory, obtaining a steady state current is almost impossible for highly insulating polymers [4]. In the present paper, a bipolar charge transport (BCT) model [5] has been used to evaluate and understand the differences in results arising from the variation of time under voltage application from seconds to quasi-steady state, and the differences arising from the experimental protocol. The BCT model has then been used with different physical hypotheses related to injection, mobility and trapping, hopefully in the spirit of [6], in order to observe the impact on the simulated current density-voltage characteristics, particularly on the reproduction of a specific S-shape, as predicted by the SCLC theory. Hypothesis of a field dependent mobility seems more appropriate to obtain an electric field threshold in the range of the experimental ones, i.e. 40 kV/mm for LDPE [5]. However, it goes against obtaining a third region in the J-E characteristic. Although many hypotheses for the mobility rule were tested in the present paper, it was not possible to correctly reproduce the experimental J-E characteristic, for a simple material such as LDPE.

II. MODEL DESCRIPTION

A bipolar charge transport model, already reported in the literature [5, 7-9], has been used for the simulations in a low density polyethylene (LDPE). This charge transport model, also called mesoscopic model in the literature for insulating polymers [10], is a hydrodynamic model, based on the advection equation. The model is one dimensional, function of the depth in the sample, and features generation of electronic charges (i.e. electrons and holes) through injection at each electrode, charge transport within the bulk, trapping into one level of deep traps, from which charges can detrapp, and charge recombination between carriers of opposite sign (Figure 2). The equations to solve are of the form:

$$\frac{\partial n_a}{\partial t} + \nabla \cdot (n_a \mu_a E - D_{diff-a} \nabla n_a) = s_a \quad (1)$$

$$\nabla \cdot (\epsilon_0 \epsilon_r E) = (qn_{h\mu} + qn_{ht} - qn_{e\mu} - qn_{et}) = \rho \quad (2)$$

Where n_a is the density (m^{-3}), and a refers to the charge carrier, being electron (e) or hole (h), mobile (μ) or trapped (t). t is the time, μ the mobility ($m^2/V/s$), for each charge carrier, E the electric field (V/m), ϵ_0 is the vacuum permittivity, and ϵ_r the relative permittivity of the material (2.3 in the case of LDPE), q is the elementary charge (C), and ρ the net charge density (C/m^3).

D_{diff-a} refers to the diffusion coefficient, and is of the form, following the Einstein relation:

$$D_{diff-a} = \frac{k_B T}{q} \mu_a \quad (3)$$

With k_B the Boltzmann's constant (J/K) and T the temperature (K). This expression of diffusion is adopted since used in organic semi-conductors, even if it is not clear whether or not it is usable when the mobility is field dependent. This particular point has been largely documented in the literature for organic semi-conductors [11,12].

s_a in (1) are the source terms, reflecting all the physical processes taken into account but not linked to transport

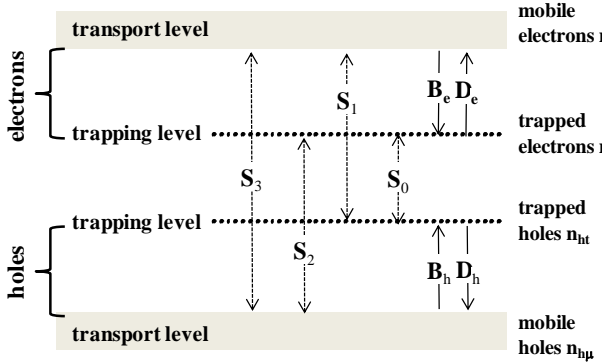


Fig. 2. Schematic representation of the bipolar charge transport model. Conduction is by free charges in the transport levels, associated with trapping and detrapping into one level of deep traps, and recombination between charge of opposite sign.

(trapping, detrapping and recombination in the present paper). An example of source term for mobile electrons is given in:

$$s_{e\mu} = -B_e n_{e\mu} \left(1 - \frac{n_{et}}{N_{0et}}\right) + D_e n_{et} - S_1 n_{e\mu} n_{ht} - S_3 n_{e\mu} n_{h\mu} \quad (4)$$

B_e is the trapping coefficient (s^{-1}), N_{0et} the trap density for electrons (m^{-3}), which corresponds to a maximal trapped charge density of $100 C/m^3$. D_e is the detrapping coefficient for electrons (s^{-1}), and S_1 and S_3 are recombination coefficients (m^3/s). The same kind of equation holds for trapped electrons and mobile and trapped holes, and can be found in [5].

All the variables are function of space and time, even if equations (1-4) do not reflect this, for sake of simplicity.

Charge generation is only due to injection of carriers at each electrode, and follows a Schottky law:

$$j_{Schott}(X) = AT^2 \exp\left(\frac{-qw_{ai}}{k_B T}\right) \left[\exp\left(\frac{q}{k_B T} \sqrt{\frac{qEX}{4\pi\epsilon_0\epsilon_r}}\right) \right] \quad (5)$$

A is the Richardson's constant, w_{ai} is the injection barrier height, for electrons or holes (eV), and the coordinate X refers either to the anode or to the cathode. There is no extraction barrier at the cathode for holes and at the anode for electrons.

The total external current density is calculated based on the following Maxwell equation:

$$J_{tot}(t) = \frac{1}{D} \int_0^D j_{cond}(x, t) dx + \epsilon_0 \epsilon_r \frac{\partial E(x, t)}{\partial t} \quad (6)$$

Where $j_{cond}(x, t)$ refers to the conduction current, being the sum of the conduction current of each mobile carrier, and D is the sample thickness.

In the present paper, the sample considered is a LDPE of thickness $150 \mu m$. The model, developed with COMSOL Multiphysics® uses the mathematic module (Partial Differential Equation) to solve the convection-diffusion equation for each kind of carrier (4 kinds). The Poisson equation module is used to couple these equations to the Poisson's equation. The Backward Differentiation Formula solver is used for the time integration (maximum order 2, and minimum order 1).

III. IMPACT OF THE APPLIED VOLTAGE PROTOCOL ON THE J-E RESULTS

A. Impact of the time under voltage application

Simulations have first been performed to observe the impact of the time of voltage application on the current density vs. electric field (J-E) characteristic. The physical hypotheses taken into account are: a constant mobility, a constant trapping coefficient, a detrapping coefficient function of temperature, for each kind of carrier, and constant recombination coefficients. A Schottky injection law (5) is used for charge generation at each electrode. An optimized set of parameters has been previously determined in [5]. Although no experimental data will be presented in the present paper, the optimized set of parameters chosen is able to reproduce most of the space charge and current measurements available for LDPE, for different experimental protocols. This set of parameters is presented in Table I and used for the simulations in section 3. The experimental protocol is a step increase of voltage, from 10 to 500 kV/mm, by steps of 10

TABLE I
Parameters used for the simulations

Symbol	value	units
Trapping coefficients		
B_e electrons	$1 \cdot 10^{-1}$	s^{-1}
B_h holes	$2 \cdot 10^{-1}$	s^{-1}
Constant mobility		
μ_e for electrons	$1 \cdot 10^{-14}$	$m^2/V/s$
μ_h for holes	$2 \cdot 10^{-13}$	$m^2/V/s$
Trap densities		
N_{tot} for electrons	$6.25 \cdot 10^{20}$	m^{-3}
N_{tot} for holes	$6.25 \cdot 10^{20}$	m^{-3}
Injection barrier heights		
w_{ei} for electrons	1.27	eV
w_{hi} for holes	1.16	eV
Recombination coefficients		
S_0, S_1 and S_2	$6.4 \cdot 10^{-22}$	m^3/s
S_3	0	m^3/s
Detrapping barrier heights		
w_{tr} for electrons	0.96	eV
w_{th} for holes	0.99	eV

kV/mm from 10 to 100 kV/mm, and by steps of 50 kV/mm from 100 to 500 kV/mm. The time between each step of voltage has been varied from $\Delta t=60$ s to 10800 s (i.e. 3 hours).

These time values are based on practices reported in the literature for polyolefins [13-21]. This leads to a total time of experiment varying from 18 min to 54 hours. Figure 3a presents the J-E characteristics for this applied voltage protocol. It is to note that the value taken to plot the J-E characteristic is the mean of the current density over the last minute under the given applied field. In the literature for experimental results, the Authors either take the last value under a given applied voltage [22], or they take the mean value over the last minutes of experiment [15-19]. For all the simulated time steps apart from 60 s, the J-E characteristic has a specific SCLC shape (or S-shape). The first region, with ohmic regime at low electric field, is not observed, but the other regions, as defined by the SCLC theory (trap-limited conduction, the trap filled limit and the trap free conduction) are observed, though the hypotheses behind the two approaches are clearly different. The impact of the time between two voltage steps on the current density values is important for times up to 600 s. On the contrary, the characteristic is almost unchanged for times above 1800 s, and the current density should have reached a quasi-steady state. This is however not totally true, and simulations results obtained with a stationary BCT model [23], with the same optimized set of parameters, presented also on Figure 3a, show a perceptible difference in the current values. The characteristic however presents the same slopes for a steady state and unsteady states. Figure 3b presents the current density as a function of time for an applied electric field of 60 kV/mm, for the different resting times between two steps. The current density at 60 kV/mm has the same characteristic for all resting times, i.e. it increases and reaches a maximum after around 20 s, and then decreases. The differences arise from the value of the current density at the beginning of the step, which is really higher (by up to one decade) for short times under voltage compared to longer ones. In all cases, the current density is still decreasing and has not reached a steady state when the next step in voltage is applied. Charges, being present due to the

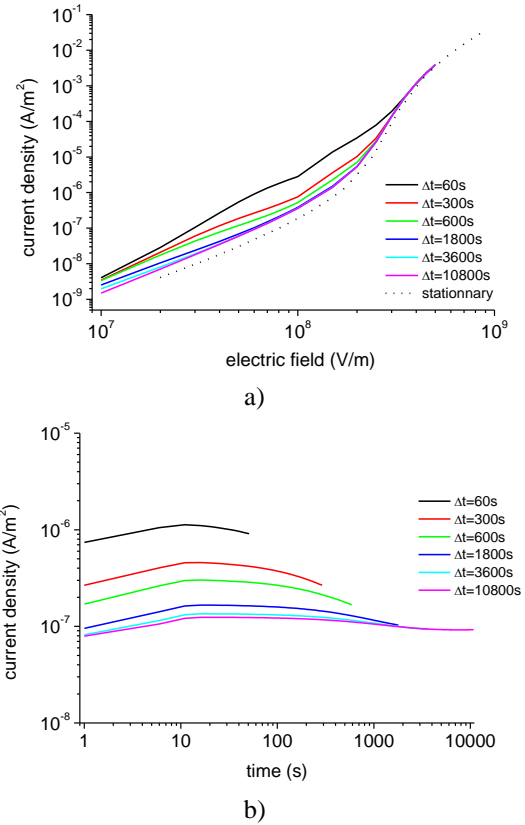


Fig. 3. a) Current density as a function of applied electric field for a step increase of voltage protocol and b) current density as a function of time for an applied electric field of 60 kV/mm, for different times between two steps.

previously applied voltages or injected at this step, have not achieved an equilibrium, leading to a high current value at the beginning of the next step of applied voltage. This behavior holds for applied electric fields ranging from 10 to 150 kV/mm. Above this field value, there is a slowing down of the differences between each resting time (Fig. 3a). It is to note that the electric field range for which there is a sharp increase of the current density is relatively high (around 200 kV/mm) compared to what is observed experimentally for a LDPE (around 60 kV/mm). This is all the more surprising that the simulation parameters have been optimized for LDPE sample with different experimental protocols, for which the step increase of voltage is one such [5]. However, during parameters optimization, the objectives were more to quantitatively reproduce most of the experimental data available, letting apart the specific SCLC shape that was not reproduced. One of the possible reasons proposed in [5] was that the mobility of holes was relatively high, making it more difficult for charges to be trapped. In the following section, simulation results are presented with different physical hypotheses, among them electric field dependent mobilities, to see their impact on the J-E characteristics.

The present simulated results show that waiting for more than 30 min between two steps is a minimum to obtain a correct value of the current density as regards stationary state, for this

specific step increase of voltage protocol and for the current physical parameters values.

B. Impact of the applied voltage protocol

Simulations have then been performed for a polarization/depolarization protocol, for the same applied voltages and different polarization times, in order to investigate the impact of the voltage application protocol on the J-E characteristic. In the previous section, a step increase of voltage has been chosen, which implicitly takes into account the state of charges at the end of the previous step of voltage. In the case of a polarization/depolarization scheme, a new sample is used for each measurement, i.e. the sample is considered free of charges before any voltage application. Figure 4a presents the simulated current density as a function of the applied electric field distribution in the material prior to field application. The net charge density is null at the beginning of the simulation for a polarization/depolarization protocol, while charges are already present and mostly decrease the electric field distribution next to the electrodes in the case of a step-increase of voltage. Hence, in the first case, there is a high generation rate, a large charge redistribution, leading to a large current transient. The current density converges faster toward a stationary state when a step increase of voltage protocol is applied, i.e. when charges are already present within the material.

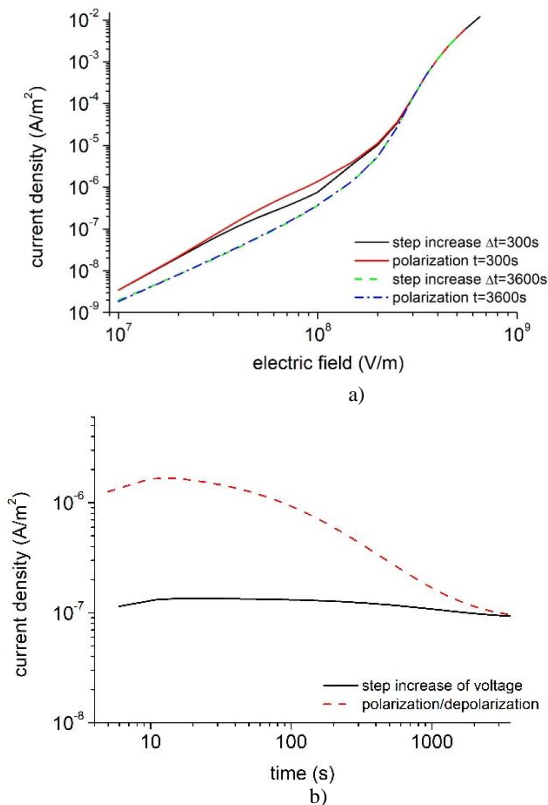


Fig. 4. a) Current density as a function of applied electric field for a polarization/depolarization protocol and different times under voltage application; b) Current density as a function of time for a step –increase of voltage and a polarization/depolarization protocol, for an applied electric field of 60 kV/mm.

leads to a large error in the estimated permittivity, as an example, in the case of a Schottky or Poole-Frenkel (PF) hypothesis, where the permittivity is directly deduced from the J-E slope.

Moreover, even if the current values are globally comparable, this does not mean that the current transients are similar during polarization. As an example for medium applied electric fields (60 kV/mm), the global behavior (see Figure 4b) presents a rising current density to reach a maximum, and then a decrease and a stabilization, for both protocols. The amplitude is however different, as for the polarization/depolarization protocol, the increase and decrease of the current is over one decade, while the current density variation in time for the step-increase of voltage protocol is of the order of 10%. This behavior is due to the charge distribution, and hence electric field distribution next to the electrodes in the case of a step-increase of voltage. Hence, in the first case, there is a high generation rate, a large charge redistribution, leading to a large current transient. The current density converges faster toward a stationary state when a step increase of voltage protocol is applied, i.e. when charges are already present within the material.

According to the model, the magnitude of the current is produced with relatively short resting times between two step-increase of voltage (>30 min). It is clear that the recommended charging time holds for the particular physical model considered here, and its parameterization. Changing material to a more resistive one would certainly require longer stabilization time.

IV. IMPACT OF THE PHYSICAL HYPOTHESES ON THE J-E RESULTS

It has been noticed before that the range of electric field at which the simulated current density value sharply increases (corresponding to V_{TFL} in Figure 1) is high (around 200 kV/mm) compared to experimental data related to LDPE (40-60 kV/mm). In this section, physical hypotheses related to injection, mobility, trapping, detrapping and recombination have been tested in order to observe their impact on the J-E characteristics. One of the objectives is to determine if this increase of current density could be reproduced for all the proposed physical hypotheses, as the choice of different physical processes can lead to the same simulated result. The second objective is to see if the threshold in electric field could be shifted to lower field values with a change of physical hypotheses (or mathematical expressions).

A. Impact of the mobility equation

Simulations have been performed for different physical hypotheses on the mobility for electrons and holes. The experimental protocol is a step-increase of voltage, for $\Delta t=1800$ s, which is not far from a stationary state as concluded in paragraph III.1. As a reference, mobility has been set as constant, with an effective constant value taking into account the possible trapping and detrapping of carriers into shallow traps (values of Table 1). A hopping mobility and a Poole

Frenkel (PF) mobility for electrons and holes have also been tested, in order to see their impact on the J-E characteristics. It is to note that the PF mobility is associated with the necessary presence of ionizable centers localized in the band gap able to release an electron in the conduction band (respectively to accept an electron, i.e. to create a hole in the valence band). These ‘donor’ or ‘acceptor’ states (as in the semi-conductor domain) would require too much energy to detrapp a carrier in the case of dielectrics, so the PF mobility is not well fitted for our materials. However, the goal here is to have a second field-dependent mobility equation, to evaluate if the current-voltage characteristics could be reproduced.

Equations and parameters used for each mobility equation are given in Table II. The other parameters of the model (related to injection, trapping, detrapping, and recombination) have been untouched and are the ones of Table I. Figure 5 presents the J-E characteristics for the different simulations using different mobility laws. The Schottky injection current for holes (having the lowest injection barrier, i.e. the higher injected current) has also been plotted vs. applied field on Figure 5, for comparison purpose. At low applied electric fields, the external currents are clearly lower than the injection current for all mobility hypotheses, i.e. the current density is not driven by the injection process. Of course, the choice of parameters for these mobility equations drives the value of the current at low fields. However, for the cases of field dependent mobility, i.e. hopping and Poole-Frenkel, the current density progressively tends to the Schottky current, whatever the chosen parameters. This means that the injection process rapidly determines the current density, for field dependent mobility cases study. For field dependent mobility equations, the increase in the current density appears at relatively low to middle applied electric fields (30 kV/mm for PF, and around 50 kV/mm for a hopping mobility), which is more consistent with experimental data than for a constant mobility. However, in the cases of field dependent mobility, with the chosen parameters as regards trapping, detrapping and recombination, the third zone of the SCLC characteristic (‘trap free region’) is not visible, and the current is always following the Schottky current. Other simulations (not presented in the present paper) have been performed with a different trap distribution (i.e. exponential [24]), and with a power-law for the field dependence of mobility [25], with adapted parameters to have current densities of the same amount as the ones obtained with a constant mobility at 10 kV/mm. These simulations, with

TABLE II
Mobility hypotheses tested in the simulations

Mobility law	Equation	parameters
Constant	μ_{const}	$\mu_e=10^{-14} \text{ m}^2/\text{V/s}$ $\mu_h=2.10^{-13} \text{ m}^2/\text{V/s}$
Hopping	$\mu_{hop} = \frac{2\lambda v}{E} \exp\left(-\frac{\varphi_{hop}}{k_B T}\right) \sinh\left(\frac{e\lambda E}{2k_B T}\right)$	$\lambda_e = \lambda_h = 3 \text{ nm}$ $v = 6.2 \cdot 10^{12} \text{ s}^{-1}$ $\varphi_{hop-e} = 0.66 \text{ eV}$ $\varphi_{hop-h} = 0.6 \text{ eV}$
Poole-Frenkel	$\mu_{PF} = \mu_0 \exp\left(-\frac{\varphi_{PF}}{k_B T}\right) \exp\left(\frac{e}{k_B T} \sqrt{\frac{eE}{\pi\epsilon_0\epsilon_r}}\right)$	$\mu_{0e} = \mu_{0h} = 10^{-6} \text{ m}^2/\text{V/s}$ $\varphi_{PF-e} = 0.66 \text{ eV}$ $\varphi_{PF-h} = 0.6 \text{ eV}$

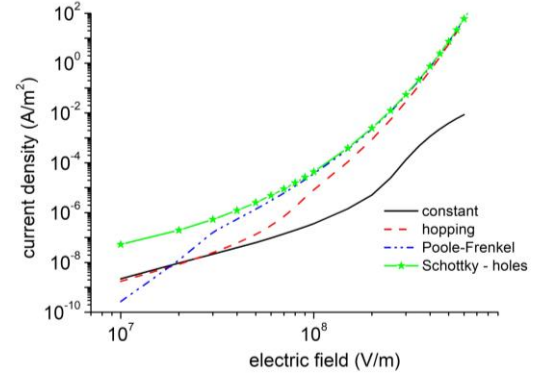


Fig. 5. Current density as a function of applied electric field for different mobility laws proposed in Table II. Other parameters as in Table I. Schottky injection is also presented for comparison.

field dependent mobility equations, lead to the same Schottky current values in the case of medium to high electric fields. As all other physical processes (injection, trapping, detrapping and recombination) and parameter values are identical, it seems that the value of the mobility in the case of a constant mobility prevents the total current from achieving the Schottky injection current. This has been already described in [23], and is directly linked to the balance of charge density between mobile and trapped charges, as predicted by the SCLC theory.

In the case of a constant mobility, the mobile charge density for electrons and holes is higher than the trapped charge density, with a trapped charge density being close to its maximal value, i.e. 100 C/m^3 . In the case of a hopping and a PF mobility, the mobile charge density is lower than the trapped one, with values for mobile and trapped charges being very low (lower than 10^{-3} C/m^3). In this case, for high electric fields, mobile charges have a high mobility, so their density is low, and the trapped charge density is also low. Hence, the electric field is no more disturbed by the charges. The current is then controlled by the electrodes. It is to note that there is quasi no difference between the simulation results obtained with the PF mobility and the one obtained for a Schottky injection, whatever the applied electric field (Figure 5). It seems that the PF mobility rapidly achieves high values, hence the current remains determined by injection. The same kind of conclusions has been reported in [25], i.e. the PF process, even with different parameters, cannot reproduce the space charge behavior at high applied electric fields.

B. Impact of the injection law

Simulations have then been performed for different injection laws, as proposed in Table III: a Schottky injection, an infinite reservoir of charges, and a Fowler-Nordheim (F-N) injection. The validity of an infinite reservoir of charges is questionable: one should account for more detailed physical hypotheses at the interface such as the presence of contact charges at each electrode, the presence of a higher density of traps, on deeper levels, etc. These charges (trapped mainly) should constitute a reservoir of charges. Moreover, one should account for the replenishment of this reservoir of charges, which is hence not constant, being depleted when relatively high fields are applied [26]. As it is difficult in reality to account for all these physical

TABLE III
Injection laws tested in the simulations

injection law	Equation	parameters
Schottky	$AT^2 \exp\left(\frac{-ew_{ai}}{k_B T}\right) \left[\exp\left(\frac{e}{k_B T} \sqrt{\frac{eE}{4\pi\epsilon_0\epsilon_r}}\right) \right]$	$\phi_{\text{Sch-e}}=1.27 \text{ eV}$ $\phi_{\text{Sch-h}}=1.16 \text{ eV}$
Fowler-Nordheim	$\frac{E^2 e^3}{8\pi h \phi_{FN}} \exp\left[-\frac{4}{3} \left(\frac{2m}{\hbar^2}\right)^{\frac{1}{2}} \frac{\phi_{FN}^3}{eE}\right]$	$\phi_{\text{FN-h}}=1.16 \text{ eV}$ $\phi_{\text{FN-e}}=1.27 \text{ eV}$
Reservoir of charges	$j_{\text{res.}} = n_{\text{res.}} \mu . E$	$n_{\text{res-h}}=300 \text{ C/m}^3$ $n_{\text{res-e}}=100 \text{ C/m}^3$

processes (no information, no parameters) we choose the simplest hypothesis, being the constant reservoir of charges, i.e. injection is not limited. For each hypothesis on injection, a constant mobility and a hopping type mobility have been tested (parameters of Table 2). Other parameters are the ones of Table I. Figure 6 presents the simulated current density as a function of applied electric field for the different cases study. The Schottky and Fowler-Nordheim injection current densities vs. applied electric field values, have also been plotted for a barrier height of $w=1.16 \text{ eV}$. In the case of a constant mobility at low to medium applied electric fields (1-100 kV/mm), when a sufficient number of charges are injected inside the dielectric (i.e. case of a reservoir of charge and Schottky injection), the current density is limited by bulk processes. The current is lower than 10^{-15} A/m^2 in the case of a F-N injection, as the number of charges injected at low field is quasi null at these applied electric fields. It means that the current for this case, at low applied electric field, is limited by the F-N injection process. At high applied electric fields, and still for a constant mobility, the current remains the same whatever the injection law, i.e. the current is still driven by the ‘low’ value of the mobility. The case of an electric field dependent mobility is more complex to comprehend. The F-N injection law implies a low current density at low applied electric fields, as in the case of a constant mobility. The current density then increases drastically with the increase of the applied electric field. At high field ($>100 \text{ kV/mm}$), the current density value follows the one

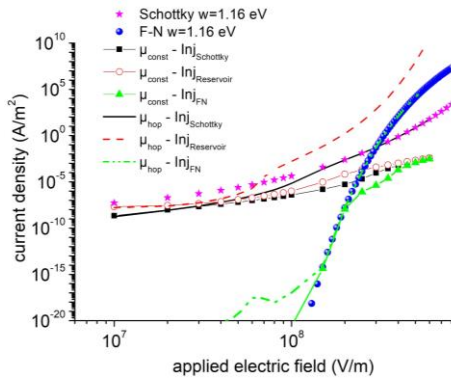


Fig. 6. Current density vs. applied electric field for different injection laws and different mobility hypotheses. Parameters as in Table II for mobility and Table III for injection. Other parameters as in Table I.

of the injection current in the case of a Schottky and a Fowler-Nordheim injection. The case of a reservoir of charges associated to a hopping mobility shows a drastic increase of the current density at high applied electric fields compared to other cases, leading to a conclusion different from a constant mobility, as the mobility does not limit the current value. For these cases study for high applied electric fields, the controlling process in the case of a constant mobility is the transport, while it is the injection in the case of a hopping mobility.

C. Impact of recombination

The impact of recombination law on the J-E characteristic has also been investigated, for the different mobility hypotheses proposed in section 4.1. Three cases have been tested, i/ constant recombination parameters, ii/ Langevin recombination, function of the mobility of the carrier, and iii/ no recombination. Figure 7 presents the current density as a function of the applied electric field for the nine different cases. Practically no differences are observed for the cases where the mobility is field dependent, whatever the recombination hypothesis, even no recombination. The only case where recombination plays a non-negligible role is when the mobility is constant. For this hypothesis, considering constant or Langevin recombination almost leads to the same current density values. A difference exists only when no recombination is considered. In that case, the current shape tends to the Schottky injection current. This particular behavior has already been highlighted in [23].

D. Impact of the trapping physical hypotheses

One last physical process, the trapping, has been investigated. For these simulations, mobility for electrons and holes are of the hopping type, as it seems more physically sound to have a field dependent mobility. Three parameters are linked to the trapping: the trapping coefficient, the trap density, which is usually kept at $6.25 \cdot 10^{20} \text{ m}^{-3}$ (producing maximal trapped charge of 100 C/m^3) in most of the researches linked to BCT models [6,8], and the detrapping barrier height. In the present research the trapping coefficient value has been changed equally for electrons and holes, from 0.1 to 100 s^{-1} . The trap density for electrons and holes has been increased from $6.25 \cdot 10^{20} \text{ m}^{-3}$ to $6.25 \cdot 10^{22} \text{ m}^{-3}$. At last, the detrapping coefficient has

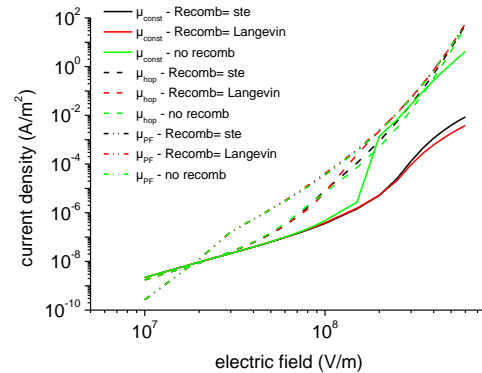


Fig. 7. Current density as a function of applied electric field for different mobility and recombination hypotheses. Other parameters as in Table I.

been varied symmetrically from 0.8 to 1.2 eV. Figure 8 presents the simulation results. Whatever the coefficient, the impact is almost the same. As stated in the SCLC theory, the trapping processes are directly related to the trap-filled limited current as in Fig. 1 (i.e. $J \propto V^\infty$, when traps are not distributed). An increase of the density of trapped charges (through an increase of the trapping coefficient B , an increase of N_0 or an increase of the detrapping barrier height) implies a decrease of the current density at low applied electric fields, a shift of the threshold in electric field to the right, i.e. toward higher values of applied electric fields, and an increase of the slope of the characteristic for medium applied fields. There is hence a clear effect of the trapping parameters on the variation of the current density at low to relatively high fields. At high applied electric fields, all the curves tend to the same current value, which is the Schottky current for holes (i.e. for a barrier height of 1.16 eV), and all the charge densities (not presented here) are low.

E. Discussion

Current density vs. electric field characteristics with a constant mobility and optimized parameters lead to unrealistic thresholds in electric fields regarding the space charge limited and trap free conduction regime (corresponding to V_{TFL} in the SCLC theory) compared to experimental data for LDPE. One of the objectives of this paper was to find how to shift the threshold in electric field to obtain simulation data fitting to experimental ones. To do so, different physical hypotheses and/or mathematical expressions have been tested. Important remarks can be deduced from the simulations in section 4:

- When the mobility is field dependent, the threshold in field approaches the one observed experimentally (around 60 kV/mm in the case of LDPE). However, keeping the optimized parameters as for a constant mobility, the trap free conduction as proposed by the SCLC theory and observed experimentally is not reproduced. Moreover, when adopting electric field dependent mobility equations, the space charge behavior cannot be reproduced, as at high applied electric fields, the amount of charges is quasi null (lower than 10^{-5} C/m³), not representative of what is experimentally observed.

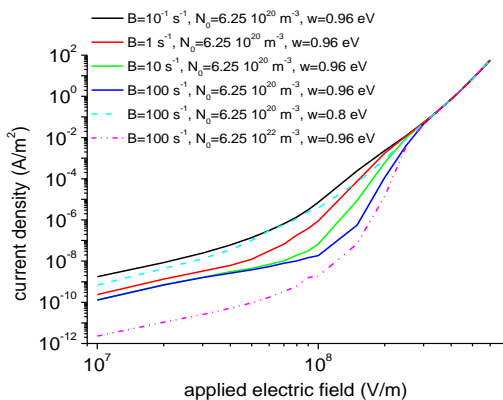


Fig. 8. Current density as a function of applied electric field for different values associated to trapping processes. Other parameters as in Table I.

- Only a constant mobility ‘respects’ the trap filled region, as presented in [23], i.e. all traps are filled, and the current is driven by bulk transport.

- When the mobility is field dependent, the current limiting step at high applied electric fields is the injection process, for the tested physical hypotheses. Changing the injection hypothesis has then a significant impact on the high field current densities. This is not the case when a constant mobility is accounted for.

- Recombination (constant or mobility dependent) has an impact only for constant mobility; the impact is negligible for field dependent mobility equations.

- Changing the trapping physical hypotheses has been performed only by changing the parameters values. It does not affect the shape of the characteristic to a large extent, but the variations on the current density values are large at low applied electric fields.

Changing the mobility equation from constant to electric field dependent has then a substantial impact on the J-E characteristic. Similar simulations, performed on semi-conducting materials [27], with an exponential and a Gaussian trap distribution, led to the same kind of conclusions, i.e. the trapping parameters are of most importance, and have to be modulated in order to change the slopes and ranges of the J-E curve. It is however difficult to shift the field threshold without changing the permittivity or the material thickness. Moreover, these simulations [27] also led to the conclusion that the injection mechanism determines the current value at high applied electric fields.

From the present results, it seems that changing the mobility law allows obtaining consistent results as regards the current density values, but the shape of the characteristic is not correct. Hence, in its current form, the BCT model is yet not enough to reproduce most of the experimental data available for LDPE, the simplest polymer in its structure. The alternative mathematical or physical hypotheses explored in the present work for such model did not lead to definitive improvement: no hypothesis as regards generation, transport, trapping has been able to reproduce at the same time an electric field threshold at a reasonable applied electric field, and a third region in the J-E characteristic, where most of the traps are filled. A possible reason could be that the real physical processes are a combination of the previously proposed ones: for example, the charge injection rule can be changing from one process to another with increasing the electrode field, or the mobility can switch from a constant to field-dependent one above a threshold. Another possibility is that the physical hypotheses chosen in the present paper are not well adapted to reproduce the experimental behavior. The present model has the advantage of dissociating all relationships between parameters of each physical process. This is however not true in reality, and evolutions of the model should certainly account for that. Other tracks, particularly as regards the trapping/detrapping hypotheses, need also to be investigated, such as for example field dependent trapping/detrapping processes or a modulation of the trapping/detrapping processes as a function of the already trapped density of charges.

III. CONCLUSIONS

A bipolar charge transport model has been used in order to evaluate the impact of each physical process, related to injection, transport and trapping, on the J-E characteristic, for a low density polyethylene. The protocol for voltage application (step-increase of voltage or simple polarization/depolarization protocol) does not seem to be critical as long as the time under a specific voltage is long enough. It has been found that for a polarization time longer than 30 min, the current values do not change to a large amount compared to steady state simulated currents. This time under voltage should then be used as a minimum for any measurement if current-voltage characteristic is under study, for the dynamics of processes considered in the present model. The charge dynamic and the current transient for each protocol (step increase of voltage and polarization/depolarization protocol) is however different, and a richer information can be deduced from polarization/depolarization protocol, compared to a step-increase of voltage protocol with combining current measurements and space charge distribution measurements. Injection, mobility, trapping and recombination have then been analyzed, to see their impact on the J-E characteristics, and particularly on the electric field threshold linked to the space charge limited current. For the physical hypotheses tested in the present paper, injection is always the dominant process when field dependent mobility is accounted for, at medium to high applied electric fields. Parameters linked to trapped charges (i.e. trapping and detrapping coefficients and trap density) have a significant impact on the shape of the characteristic when field dependent mobility is accounted for, leading to a S-shape characteristic in the case where enough charges can be trapped, but with thresholds in electric field far from the ones observed experimentally for LDPE. More work needs to be done on the mathematical expressions and/or on the physical hypotheses that need to be implemented in such BCT model to have simulation results consistent with experimental J-E characteristics.

REFERENCES

- [1] H. J. Wintle, 'Absorption currents and steady currents in polymer dielectrics,' *J. Non-Crystalline Solids*, vol. 15, no. 3, pp. 471–486, 1974.
- [2] M. S. Bhutta *et al.*, 'Steady-State Conduction Current Performance for Multilayer Polyimide/SiO₂ Films,' *Polymers*, vol. 13, no. 4, 640 (15p), 2021.
- [3] H. Hamedi *et al.*, 'Impact of the Impurities on the Conductivity of Low-Density Polyethylene,' *Annu. Rep Conf. Electr. Insul. Dielect. Phenom. (CEIDP)*, 2020, pp. 13–16.
- [4] H. Ghorbani *et al.*, 'Long-term conductivity decrease of polyethylene and polypropylene insulation materials,' *IEEE Trans. Dielectr. Electr. Insul.*, vol. 24, no. 3, pp. 1485–1493, 2017.
- [5] S. Le Roy *et al.*, 'Description of charge transport in polyethylene using a fluid model with a constant mobility: fitting model and experiments,' *J. Phys. D: Appl. Phys.*, vol. 39, no. 7, pp. 1427–1436, 2006.
- [6] L.A. Dissado, 'The Role of Theory in Understanding Space Charge Distributions,' *Proc. Int. Symp. Electr. Insul. Mat. (ISEIM)*, 2020, pp 1-14
- [7] J. M. Alison and R. M. Hill, 'A model for bipolar charge transport, trapping and recombination in degassed crosslinked polyethene,' *J. Phys. D: Appl. Phys.*, vol. 27, no. 6, pp. 1291–1299, 1994.
- [8] J. Xia *et al.*, 'Numerical analysis of packetlike charge behavior in low-density polyethylene by a Gunn effectlike model,' *J. Appl. Phys.*, vol. 109, 034101 (9p), 2011.
- [9] A. T. Hoang, Y. V. Serdyuk, and S. M. Gubanski, 'Charge Transport in LDPE Nanocomposites Part II—Computational Approach,' *Polymers*, vol. 8, 103 (16p), 2016.
- [10] E. Doedens *et al.*, 'Space Charge Accumulation at Material Interfaces in HVDC Cable Insulation Part I—Experimental Study and Charge Injection Hypothesis,' *Energies*, vol. 13, 8 (16p), 2020.
- [11] G. A. H. Wetzelaer, L. J. A. Koster, and P. W. M. Blom, 'Validity of the Einstein relation in disordered organic semiconductors,' *Phys. Rev. Lett.*, vol. 107, 0666605, 2011.
- [12] A B Walker A. Kambili and S.J. Martin, 'Electrical transport modelling in organic electroluminescent devices', *J. Phys.: Condens. Matter*, vol. 14, pp. 9825-9876, 2002
- [13] K. Hashimoto *et al.*, 'Space Charge and Conduction Current in Polypropylene Based Material Added Inorganic Filler under DC High Stress', *Annu. Rep Conf. Electr. Insul. Dielect. Phenom. (CEIDP)*, 2019, pp. 462–465.
- [14] K. Kadowaki *et al.*, 'Observation of current spikes caused by possible fast carrier transport through a low-density polyethylene sheet under high DC fields', *Jpn. J. Appl. Phys.*, vol. 57, 03EG08 (5p), 2018.
- [15] G. Teyssedre *et al.*, 'Charge distribution and electroluminescence in cross-linked polyethylene under dc field', *J. Phys. D: Appl. Phys.*, vol. 34, no. 18, pp. 2830–2844, 2001.
- [16] R. Su *et al.*, 'Investigation of effects of charge injection and intrinsic ionic carriers in low-density polyethylene and cross-linked polyethylene', *J Appl. Phys.*, vol. 127, 165103 (9p), 2020.
- [17] M. Chen *et al.*, 'Space charge dynamics of acetophenone and cumyl alcohol and their synergistic effect in LDPE', *IEEE Trans. Dielectr. Electr. Insul.*, vol. 27, no. 1, pp. 67–75, 2020.
- [18] D. Li *et al.*, 'Effect of Crystallinity of Polyethylene with Different Densities on Breakdown Strength and Conductance Property', *Materials*, vol. 12, 1746 (13p), 2019.
- [19] Z. Li *et al.*, 'Trap Modulated Charge Carrier Transport in Polyethylene/Graphene Nanocomposites', *Sci. Rep.*, vol. 7, 4015 (8p), 2017.
- [20] S. Kumara *et al.*, 'Electrical Characterization of a New Crosslinked Copolymer Blend for DC Cable Insulation', *Energies*, vol. 13, 1434 (15p) 2020.
- [21] H. Yahyaoui *et al.*, 'Electrical properties of polytetrafluoroethylene with mineral fillers under high DC electric field', *Annu. Rep Conf. Electr. Insul. Dielect. Phenom. (CEIDP)*, 2017, pp. 712–715.
- [22] G. Chen *et al.*, 'Conduction in linear low density polyethylene nanodielectric materials', *Proc. Conf. Prop. Appl. Dielectr. Mat. (ICPADM)*, 2009, pp. 845–848.
- [23] F. Baudoin *et al.*, 'Bipolar charge transport model with trapping and recombination: an analysis of the current versus applied electric field characteristic in steady state conditions', *J. Phys. D: Appl. Phys.*, vol. 41, 025306 (11p), 2007.
- [24] F. Boufayed *et al.*, 'Models of bipolar charge transport in polyethylene', *J. Appl. Phys.*, vol. 100, 104105 (10p), 2006.
- [25] J. Zhao, Z. Xu, G. Chen and P. Lewin, 'Effect of field-dependent mobility on current density and dynamics of space charge in polyethylene', *Annu. Rep Conf. Electr. Insul. Dielect. Phenom. (CEIDP)*, 2009, pp. 120-123
- [26] L.A. Dissado, S. Le Roy, 'The effect of Contact Charge upon the Injection Current at an Electrode-Insulator Interface', *Proc. Int. Conf. Solid Dielectr. (ICSD)*, 2007, pp. 31-34
- [27] S.K. Kim and Y.S. Kim, 'Charge carrier injection and transport in QLED layer with dynamic equilibrium of trapping/de-trapping carriers', *J. Appl. Phys. Vol. 126*, 035704 (9p), 2019